Table 2. continued

spot no.[a]	accession no.[b]	identified protein	Wilcoxon test p value	fold difference (ratio of means)	pI (cal)[c]	MW (cal) (Da)[c]	protein score[d]	peptide matches	sequence coverage (%)
2790	P07237	protein disulfide-isomerase	1.5877×10^{-5}	0.085599608	4.76	57480	313	7	15.4
1877	P62820	Ras-related protein Rab-1A	1.5877×10^{-5}	0.086095703	5.93	22891	216	4	27.3
2971	Q12765	secernin-1	1.5877×10^{-5}	0.087093501	4.66	46980	42	1	2.7
1689	P52565	Rho GDP-dissociation inhibitor 1	1.5877×10^{-5}	0.089182867	5.02	23250	207	5	22.1
2972	Q8N7U6	EF-hand domain-containing family member B	1.5877×10^{-5}	0.089364253	7.5	94558	48	1	1.8
3085	Q99536	synaptic vesicle membrane protein VAT-1	1.5877×10^{-5}	0.090047239	5.88	42122	186	4	17
2841	Q96FT9	uncharacterized protein C14orf179	1.5877×10^{-5}	0.090304869	4.57	23572	44	1	9.1
2124	P60660	myosin light polypeptide 6	1.5877×10^{-5}	0.090851666	4.56	17090	205	4	28.5
2564	P27824	calnexin	1.5877×10^{-5}	0.09097873	4.47	67982	224	4	10.1
2030	Q9H0J4	glutamine-rich protein 2	1.5877×10^{-5}	0.091020777	6.25	181228	45	1	0.5
2839	Q13885	tubulin beta-2A chain	1.5877×10^{-5}	0.091496662	4.78	50274	279	5	11.9
1426	P84157	matrix-remodeling-associated protein 7	1.5877×10^{-5}	0.091543619	4.24	21509	48	1	3.9
992	P60709	actin, cytoplasmic 1	1.5877×10^{-5}	0.092202715	5.29	42052	359	21	21.1
1635	P67936	tropomyosin alpha-4 chain	1.5877×10^{-5}	0.093892535	4.67	28619	613	67	35.1
3441	Q92630	dual specificity tyrosine-phosphorylation-regulated kinase 2	1.5877×10^{-5}	0.094160695	9.7	67123	40	1	4
1128	P40121	macrophage-capping protein	6.3507×10^{-5}	0.094214275	5.88	38779	264	7	14.7
3328	P07339	cathepsin D	1.5877×10^{-5}	0.094241211	6.1	45037	190	4	11.2
3468	Q8WWM9	cytoglobin	1.5877×10^{-5}	0.094317704	6.32	21505	174	4	19.5
1681	P04264	keratin, type II cytoskeletal 1	0.00030166	0.094354027	8.15	66170	807	14	25.6
252	P14625	endoplasmin	1.5877×10^{-5}	0.095256618	4.76	92696	1270	75	33
863	Q07960	Rho GTPase-activating protein 1	1.5877×10^{-5}	0.095902059	5.85	50461	189	6	15.7
3481	P62820	Ras-related protein Rab-1A	1.5877×10^{-5}	0.097286337	5.93	22891	68	1	7.8
3561	P07477	trypsin-1	1.5877×10^{-5}	0.097721585	6.08	27111	67	1	8.1
1292	Q9P1Z9	uncharacterized protein KIAA1529	1.5877×10^{-5}	0.098548367	5.74	192404	43	4	1.2
3573	P07477	trypsin-1	6.3507×10^{-5}	0.098828882	6.08	27111	79	1	8.1
2009	P00441	superoxide dismutase [Cu−Zn]	1.5877×10^{-5}	0.09993381	5.7	16154	44	1	9.1
1836	P51149	Ras-related protein Rab-7a	6.3507×10^{-5}	0.101448964	6.4	23760	421	7	38.2
3263	P47756	F-actin-capping protein subunit beta	1.5877×10^{-5}	0.101659636	5.36	31616	102	2	8.7
1843	P51149	Ras-related protein Rab-7a	3.1754×10^{-5}	0.101686834	6.4	23760	262	6	37.7
2837	Q13885	tubulin beta-2A	1.5877×10^{-5}	0.101856539	4.78	50274	459	11	24
758	P14625	endoplasmin	6.3507×10^{-5}	0.101899313	4.76	92696	245	6	7.3
1492	Q9BPX1	17-beta-hydroxysteroid dehydrogenase 14	6.3507×10^{-5}	0.101946674	5.8	28642	37	1	4.4
998	P60709	actin, cytoplasmic 1	1.5877×10^{-5}	0.102092468	5.29	42052	715	90	34.1
3383	Q9Y5Z4	heme-binding protein 2	1.5877×10^{-5}	0.102129229	4.58	22861	156	3	19.5
964	Q9UNH7	sorting nexin-6	1.5877×10^{-5}	0.102531665	5.81	46905	261	6	15.3
3264	P47756	F-actin-capping protein subunit beta	1.5877×10^{-5}	0.103384254	5.36	31616	265	4	13.7
1609	Q9UL46	proteasome activator complex subunit 2	1.5877×10^{-5}	0.105128204	5.44	27515	94	2	10.9
2914	P21281	V-type proton ATPase subunit B, brain isoform	1.5877×10^{-5}	0.105169042	5.57	56807	509	12	20.5
3305	O00299	chloride intracellular channel protein 1	1.5877×10^{-5}	0.105232399	5.09	27248	262	4	21.2
1548	P06753	tropomyosin alpha-3 chain	1.5877×10^{-5}	0.105267655	4.68	32856	343	36	15.1
1583	P67936	tropomyosin alpha-4 chain	1.5877×10^{-5}	0.106071807	4.67	28619	426	9	30.2
1211	P50213	isocitrate dehydrogenase [NAD] subunit alpha	1.5877×10^{-5}	0.106662107	6.47	40022	150	3	8.5
1581	Q96C19	EF-hand domain-containing protein D2	1.5877×10^{-5}	0.107781812	5.15	26794	46	1	5
2847	Q13885	tubulin beta-2A chain	1.5877×10^{-5}	0.107841883	4.78	50274	319	6	18.9
3311	P62258	14-3-3 protein epsilon	1.5877×10^{-5}	0.108066218	4.63	29326	359	7	27.8
884	Q07960	Rho GTPase-activating protein 1	0.00071446	0.108386461	5.85	50461	291	7	10.9
2556	P14314	glucosidase 2 subunit beta	1.5877×10^{-5}	0.108738059	4.33	60357	194	4	10.2
1457	Q8N8N7	glucosidase 2 subunit beta	1.5877×10^{-5}	0.109312543	5.27	38930	40	1	2.6
2566	P27824	calnexin	1.5877×10^{-5}	0.109775315	4.47	67982	267	6	11.8
1439	P84157	matrix-remodeling-associated protein 7	1.5877×10^{-5}	0.109934952	4.24	21509	172	3	17.6
2180	P04264	keratin, type II cytoskeletal 1	1.5877×10^{-5}	0.110359174	8.15	66170	289	6	11
1247	P06748	nucleophosmin	1.5877×10^{-5}	0.110641094	4.64	32726	42	1	3.1

dx.doi.org/10.1021/pr400929h | J. Proteome Res. XXXX, XXX, XXX−XXX

Table 2. continued

spot no.[a]	accession no.[b]	identified protein	Wilcoxon test p value	fold difference (ratio of means)	pI (cal)[c]	MW (cal) (Da)[c]	protein score[d]	peptide matches	sequence coverage (%)
2214	O75916	regulator of G-protein signaling 9	1.5877×10^{-5}	0.110938705	9.42	77601	36	1	1.2
2612	P08670	vimentin	1.5877×10^{-5}	0.111308534	5.06	53676	1077	24	41.8
2286	Q96QU1	protocadherin-15	1.5877×10^{-5}	0.111433545	4.94	217303	36	1	0.6
1999	P52565	Rho GDP-dissociation inhibitor 1	1.5877×10^{-5}	0.112138698	5.02	23250	216	5	15.2
860	Q9UNH7	sorting nexin-6	1.5877×10^{-5}	0.11235212	5.81	46905	79	2	5.2
1149	P61160	actin-related protein 2	1.5877×10^{-5}	0.112416534	6.3	45017	50	1	3
3513	O60423	probable phospholipid-transporting ATPase IK	1.5877×10^{-5}	0.113222024	7.97	149532	48	1	1.6
1345	Q96JI7	spatacsin	1.5877×10^{-5}	0.113459904	5.63	282621	39	2	1
1814	P61586	transforming protein RhoA	1.5877×10^{-5}	0.113566968	5.83	22096	49	1	4.1
3180	P10809	60 kDa heat shock protein, mitochondrial	1.5877×10^{-5}	0.113616827	5.7	61187	133	3	5.2
533	P29083	general transcription factor IIE subunit 1	1.5877×10^{-5}	0.113756065	4.74	49763	41	1	3.2
3181	Q9UJ70	*N*-acetyl-D-glucosamine kinase	1.5877×10^{-5}	0.114109084	5.81	37694	224	4	14.8
3522	P84077	ADP-ribosylation factor 1	1.5877×10^{-5}	0.114951474	6.32	20741	274	6	32
2952	Q9P1U1	actin-related protein 3B	1.5877×10^{-5}	0.115291654	5.61	48090	76	1	2.6
2254	Q14005	pro-interleukin-16	3.1754×10^{-5}	0.115572204	8.34	142976	41	1	1.3
950	Q01105	protein SET	1.5877×10^{-5}	0.116088182	4.23	33469	278	5	22.8
277	P27824	calnexin	1.5877×10^{-5}	0.117230427	1	67982	584	13	5
1553	P06753	tropomyosin alpha-3 chain	1.5877×10^{-5}	0.117344658	4.68	32856	46	1	3.9
1481	Q49AM3	tetratricopeptide repeat protein 31	1.5877×10^{-5}	0.117497177	8.52	57753	42	1	2.7
1665	P63104	14-3-3 protein zeta/delta	1.5877×10^{-5}	0.119108879	4.73	27899	339	13	24.9
2840	Q13885	tubulin beta-2A chain	1.5877×10^{-5}	0.119125209	4.78	50274	91	2	8.5
498	Q16822	phosphoenolpyruvate carboxykinase [GTP]	1.5877×10^{-5}	0.119425451	7.56	71447	134	3	6.3
3331	Q5TAX3	zinc finger CCHC domain-containing protein 11	1.5877×10^{-5}	0.11952247	8.3	188014	35	1	1
3555	P16949	stathmin	1.5877×10^{-5}	0.119549402	5.76	17292	130	3	20.8
2921	P08670	vimentin	0.00215924	0.120101433	5.06	53676	320	7	14.8
2571	Q9H0J4	glutamine-rich protein 2	1.5877×10^{-5}	0.120540368	6.25	181228	45	1	0.5
3285	P08758	annexin A5	1.5877×10^{-5}	0.120737507	4.94	35971	930	21	48.1
1591	P67936	tropomyosin alpha-4 chain	1.5877×10^{-5}	0.121326925	4.67	28619	165	4	17.3
1433	Q9P1Z9	uncharacterized protein KIAA1529	1.5877×10^{-5}	0.121566905	5.74	192404	44	3	1.2
3452	P09211	glutathione S-transferase P	1.5877×10^{-5}	0.121610737	5.43	23569	205	3	21.4
1840	P51149	Ras-related protein Rab-7a	3.1754×10^{-5}	0.121913756	6.4	23760	171	4	24.6
746	P60709	actin, cytoplasmic 1	1.5877×10^{-5}	0.121964836	5.29	42052	387	11	21.3
2560	P14314	glucosidase 2 subunit beta	1.5877×10^{-5}	0.12226935	4.33	60357	230	4	8.5
1546	Q6ZMW3	echinoderm microtubule-associated protein-like 6	1.5877×10^{-5}	0.124504715	7.17	220270	38	1	0.4
3178	P07951	tropomyosin beta chain	0.00030166	8.436657849	4.66	32945	674	13	34.9
3177	P07951	tropomyosin beta chain	0.00071446	8.672066697	4.66	32945	502	9	27.5
2189	P35030	trypsin-3	0.00730333	8.755681188	7.46	33306	66	1	4.3
3124	P68133	actin, alpha skeletal muscle	0.00409621	13.86346832	5.23	42366	561	16	31.8
3123	P62736	actin, aortic smooth muscle	0.00730333	23.794185	5.23	42381	386	17	19.6

[a]Spot numbers refer to those in Figure 1B. [b]Accession numbers of proteins were derived from Swiss-Plot and NBCI nonredundant databases. [c]Theoretical isoelectric point and molecular weight obtained from Swiss-Prot. [d]Mascot score for the identified proteins based on the peptide ions score ($p < 0.05$) (http://www.matrixscience.com).

Figure 2 in the Supporting Information). We then examined the expression of SET in normal tissues using Western blotting and found that none of these tissues expressed SET (Figure 3C). We surveyed the expression of SET in different histologic types of sarcomas such as gastrointestinal stromal tumor, osteosarcoma, rhabdomyosarcoma, alveolar soft part sarcoma, and epithelioid sarcoma and found that SET was expressed to various degrees in all of them (Figure 3D).

3.3. Functional Verification of the Overexpressed SET Oncogene Product in ASPS Cells

To verify the functional significance of SET overexpression in ASPS, we performed a gene-silencing assay. Transfection of three siRNAs against SET resulted in a marked decrease in SET protein expression (Figure 4A). The cells with reduced SET expression showed significantly diminished cell proliferation relative to cells transfected with control siRNA (Figure 4B). The matrigel invasion assay showed that silencing of SET caused a significant decrease in invasion and migration of ASPS cells (Figure 4C,D). These observations suggested that SET may be involved in tumor progression in ASPS.

3.4. Apoptotic Effects of the PP2A Activator, FTY720, on ASPS Cells

SET is known to be an inhibitor of PP2A, which reduces the kinase-dependent signal transduction pathway, causing

dx.doi.org/10.1021/pr400929h | J. Proteome Res. XXXX, XXX, XXX–XXX

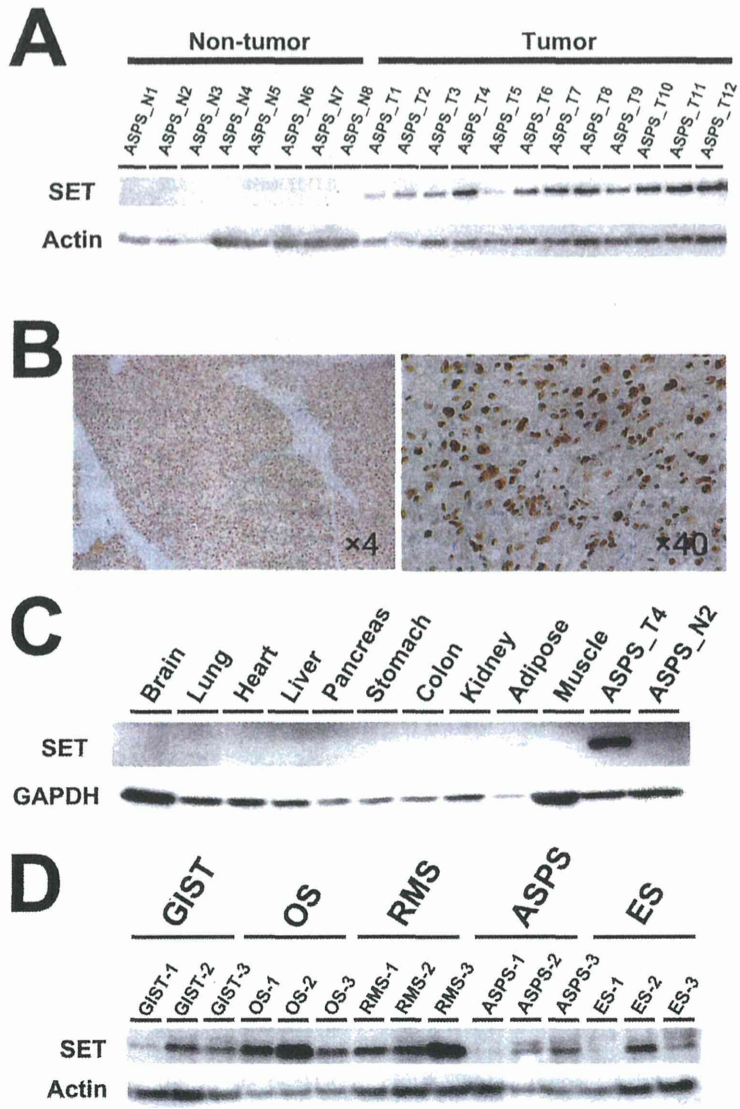

Figure 3. Immunological validation of SET overexpression in ASPS tumor cells. (A) Expression of SET was evaluated in tumor tissues and nontumor tissues by Western blotting. SET was preferentially expressed in tumor tissues. (B) Immunohistochemistry demonstrated the expression and localization of SET in tumor and nontumor tissues. Note that SET was absent in nontumor cells that surrounded tumor cells (left panel). Nuclear localization of SET is demonstrated (right panel). The results of immunohistochemistry for 15 cases of ASPS are exhibited in Supplementary Figure 2 in the Supporting Information. (C) Expression of SET in organs and tissues was evaluated by Western blotting. Note that SET expression was observed only in ASPS tumor tissues. (D) Expression of SET in sarcomas of different histologic types was assessed by Western blotting. Note that SET protein was expressed to various degrees in all of the sarcomas examined.

mitochondria-dependent apoptosis.[20] We hypothesized that the inhibitory effects of SET on PP2A would be responsible for the tumor progression of SET and that the PP2A pathway might be a novel therapeutic target in ASPS. To address this hypothesis, we examined the effects of a PP2A activator, FTY720, on ASPS cells. FTY720 is used for the treatment of patients with multiple sclerosis, and its application to anticancer therapy has been considered.[21] Treatments of ASPS cells with FTY720 markedly suppressed their proliferation in a dose- and time-dependent manner (Figure 5A,B). We found that the PP2A treatment altered the expression of proteins involved in mitochondria-mediated apoptosis, including phosphorylated Akt, Bad, and Bid (Figure 5C), consistent with previous reports.[22−24] These observations suggested the possible utility of the PP2A activator, FTY720, for treatments of ASPS.

4. DISCUSSION

ASPS is refractory to standard chemotherapy and radiation therapy, and novel therapeutic targets have long been sought to improve the clinical outcome.[25] Although proteomics is an approach worth trying for ASPS, no such study has been performed previously, probably because of the extreme rarity of ASPS and the difficulty in obtaining adequate clinical samples. In fact, in 2010, only 11 cases of ASPS were registered in Japan,[26] and gel-based proteomics such as 2D-DIGE requires frozen tissue samples, which are usually not stored in hospitals.

dx.doi.org/10.1021/pr400929h | J. Proteome Res. XXXX, XXX, XXX−XXX

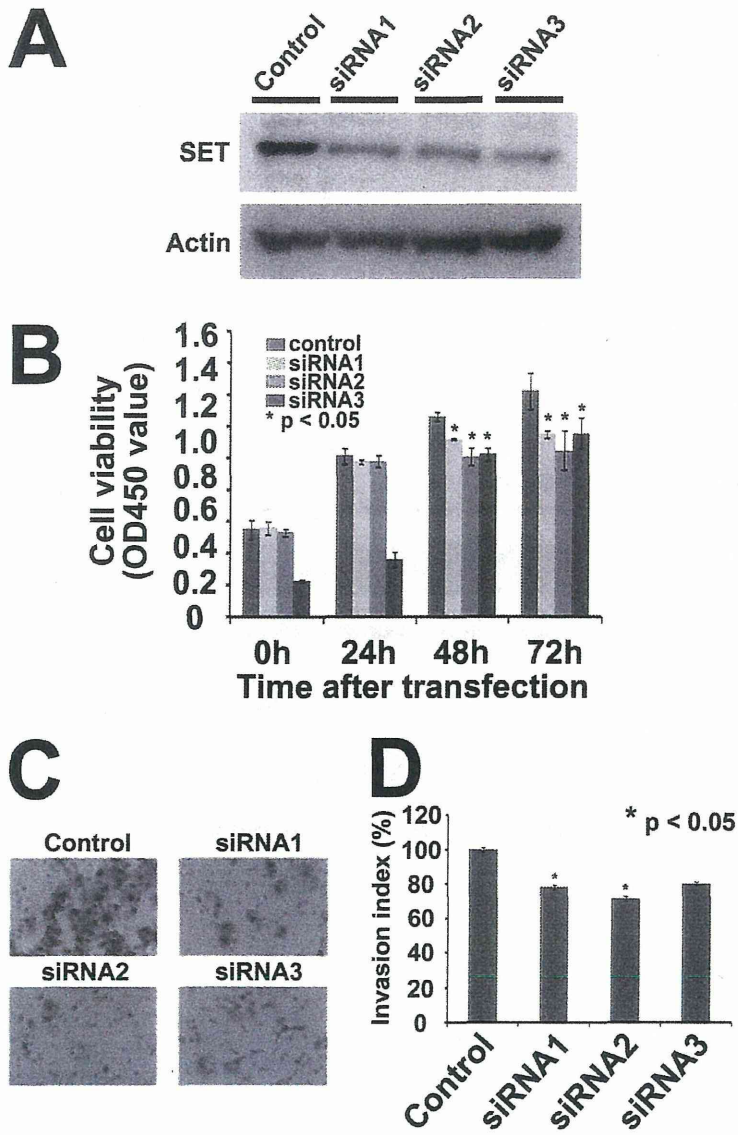

Figure 4. In vitro functional verification of SET in ASPS cells. (A) SET expression was suppressed by treatment with specific siRNAs against SET relative to treatment with control siRNA. Treatment with siRNAs 1–3 decreased the expression of SET in ASPS cells. (B) Proliferation of cells showing decreased SET expression was significantly inhibited. (C) Appearance of invading cells treated with siRNAs against SET. (D) Number of invasive cells was significantly ($p < 0.05$) decreased by treatment with siRNAs 1–3.

These issues are inherent to rare diseases and conventional proteomics methods and are an obstacle to basic research that requires the use of clinical materials. In the present study, we successfully examined 12 samples of frozen ASPS tissue and validated the results of proteomics in 15 cases, including 3 newly enrolled cases (Table 1). Because all cases of ASPS share a common chromosomal rearrangement and expression of an activated transcription factor, ASPL-TFE3,[2] the molecular background of ASPS may be homogeneous. Thus, even from a small number of samples we may be able to obtain results that would shed light on the general background of the disease.

We employed 2D-DIGE to create protein expression profiles. In 2D-DIGE, the proteins are extensively separated according to isoelectric point and molecular weight, and the levels of their expression are evaluated in terms of fluorescent signals, which have a wide dynamic range. Moreover, gel-to-gel variations are compensated for by using a common internal standard sample. We developed our own large-format gel electrophoresis apparatus, which allows wider coverage of the proteome.[27] In the present study, we observed 2300 protein spots, and normalized their intensity (Supplementary Table 2 in the Supporting Information). Together with details of the clinical parameters of the cases employed (Supplementary Table 1 in the Supporting Information), our proteome data will be useful for further studies of ASPS.

We identified higher expression of SET in ASPS tissues relative to adjacent nontumor tissues (Figure 2). Overexpression of SET was confirmed in all 15 cases of ASPS by Western blotting and immunohistochemistry (Figure 2). We found that SET was generally expressed to various degrees in sarcomas (Figure 2). The clinical significance of differences in the expression level

dx.doi.org/10.1021/pr400929h | J. Proteome Res. XXXX, XXX, XXX–XXX

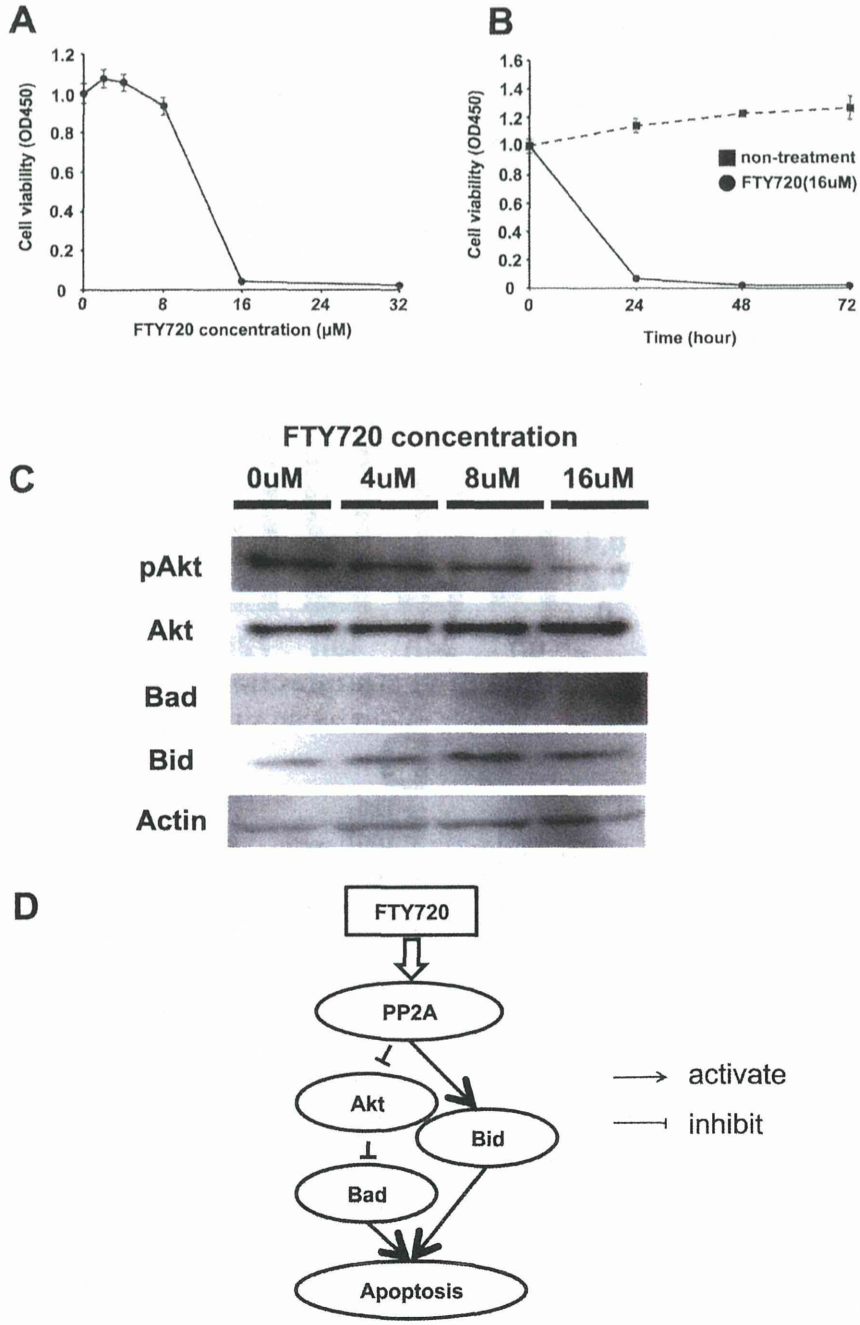

Figure 5. Effects of the PP2A activator, FTY720, on cell proliferation and apoptosis. (A) Effects of FTY720 on cell viability were examined as a function of FTY720concentration. (B) Time-dependent inhibitory effects of FTY720 (16 μM) on cell viability. (C) Effects of FTY720 at various concentrations on the expression of apoptosis-regulating proteins were examined by Western blotting. Note that treatment of the cells with FTY720 caused a reduction in the expression of pAkt and increased the expression of Bad and Bid. In contrast, Akt expression level was not affected by FTY720 treatments. These proteins were not observed by 2D-DIGE. (D) Activation of PP2A by treatment with FTY720 triggers the apoptosis pathway, resulting in reduced proliferation of ASPS cells.

of SET may be worth investigating in the context of its predictive or prognostic utility. In this study, the SET expression was observed in ASPS and the other sarcomas but not in normal tissues examined, suggesting that SET expression may represent common characters of malignancies including sarcomas.

The molecular mechanisms responsible for SET overexpression are intriguing but still unclear. ASPS is characterized by chromosomal rearrangement and expression of an activated transcription factor, ASPL-TFE3.[2] Genes under the control of this fusion gene have been revealed by DNA microarray experiments, and such genes would likely account for the molecular

dx.doi.org/10.1021/pr400929h | J. Proteome Res. XXXX, XXX, XXX–XXX

background of hyper-angiogenesis observed in ASPS.[3−5] However, SET is not one of the genes that are regulated by ASPL-TFE3.[3−5] Cervoni et al. reported overexpression of SET in various cancers such as those of the breast, uterus, colorectum, stomach, and kidney relative to their adjacent normal tissues[28] but not in ASPS. Recently, in a study of chronic myeloid leukemia, Piazza et al. found a mutation in SET binding protein 1 (SETBP1), which hindered the degradation of SET and increased the expression level of both SETBPs and SET.[29] Elucidation of the functional properties of the protein complex of SET may provide further insight into the etiology of ASPS. Because higher expression of SET is observed in a wide variety of malignancies, it may be attributable to common and important molecular mechanisms and therefore warrants further investigation. It is interesting if SET is a key to reach to common molecular backgrounds among malignancies including ASPS.

Because overexpression of SET may be a novel therapeutic target in ASPS, we focused on SET in the present study. SET is a multifunctional protein with an inhibitory effect on the activity of PP2A, which is one of the major cellular serine-threonine phosphatases[21] and negatively regulates signaling pathways such as the PI3K/Akt pathway,[30] which is aberrantly regulated in various cancers. PP2A is a tumor-suppressor protein, and its functional inactivation has been reported in several cancers.[31] Switzer et al. have reported a novel SET interactive peptide, COG112, which inhibits the association between SET and the PP2A catalytic subunit.[32] Treatment of cancer cells with CIG112 increases PP2A activity and inhibits Akt signaling and cellular proliferation. In leukemia, activators of PP2A such as forskolin,[33] 1,9-dideoxy-forskolin,[34] and FTY720[35] effectively antagonize leukemogenesis. Remarkably, even in imatinib-resistant leukemia cells, restoration of PP2A activity, either by application of a chemical PP2A activator or interference with SET/PP2A interplay, has been reported to inactivate BCR/ABL, trigger growth suppression, enhance apoptosis, and impair leukemogenesis.[36] Therefore, PP2A may be a promising drugable therapeutic target for patients who show resistance to treatment. In rare diseases, it may be difficult to develop original drugs because of their low commercial potential; therefore, additional use of existing drugs may be regarded as a more practical approach. Here we focused on FTY720 because it has been used for treatment of multiple sclerosis and malignancies.[21] We found that treatment of ASPS cells with FTY720 induced apoptosis and inhibited cell proliferation, invasion, and migration (Figure 3). ASPS exhibits MET autophosphorylation following activation of downstream signaling pathways, and the clinical efficacy of a multikinase inhibitor, sunitinib malate, has been demonstrated in ASPS.[12,13,37] Because FTY720 affects the signal transduction pathway through a mechanism differing from than of MET, it would be worth examining the utility of PP2A activator for ASPS patients who show resistance to kinase inhibitors. The effects of FTY720 on ASPS cells should be investigated further using additional cell lines and animal models.

In conclusion, we have successfully identified the expression of SET in ASPS using a proteomics approach. The possible application of PP2A activator for treatment of ASPS will be investigated further. Because overexpression of SET was generally observed in sarcomas, the application of the PP2A activators for sarcoma treatments is worth examining. To elucidate the molecular background responsible for overexpression of SET, it is essential to establish ASPS cell lines. We anticipate that our research activity will eventually be of benefit to ASPS patients.

■ ASSOCIATED CONTENT

Supporting Information

Supplementary Figure 1: Typical image of two-dimensional difference gel electrophoresis. Supplementary Figure 2: Immunohistochemistry of SET in tumor cells and non-tumor cells. Supplement Table 1: Patient's characteristics of various saroma cases Supplement Table 2: A summary of the intensity of all protein spots. Supplement Table 3: Supportive information for protein identification. This material is available free of charge via the Internet at http://pubs.acs.org.

■ AUTHOR INFORMATION

Corresponding Author

*Tel: +81-3-3542-2511. Fax: +81-3-3547-5298. E-mail: takondo@ncc.go.jp.

Notes

The authors declare no competing financial interest.

■ ACKNOWLEDGMENTS

This study was supported by the National Cancer Center Research Core Facility and by the National Cancer Center Research and Development Fund (23-A-7 and 23-A-10). Patient's characteristics of various saroma cases.

■ REFERENCES

(1) Christopherson, W. M.; Foote, F. W., Jr.; Stewart, F. W. Alveolar soft-part sarcomas; structurally characteristic tumors of uncertain histogenesis. *Cancer* **1952**, *5* (1), 100−111.

(2) Ladanyi, M.; Lui, M. Y.; Antonescu, C. R.; Krause-Boehm, A.; Meindl, A.; Argani, P.; Healey, J. H.; Ueda, T.; Yoshikawa, H.; Meloni-Ehrig, A.; Sorensen, P. H.; Mertens, F.; Mandahl, N.; van den Berghe, H.; Sciot, R.; Dal Cin, P.; Bridge, J. The der(17)t(X;17)(p11;q25) of human alveolar soft part sarcoma fuses the TFE3 transcription factor gene to ASPL, a novel gene at 17q25. *Oncogene* **2001**, *20* (1), 48−57.

(3) Lazar, A. J.; Das, P.; Tuvin, D.; Korchin, B.; Zhu, Q.; Jin, Z.; Warneke, C. L.; Zhang, P. S.; Hernandez, V.; Lopez-Terrada, D.; Pisters, P. W.; Pollock, R. E.; Lev, D. Angiogenesis-promoting gene patterns in alveolar soft part sarcoma. *Clin. Cancer Res.* **2007**, *13* (24), 7314−7321.

(4) Stockwin, L. H.; Vistica, D. T.; Kenney, S.; Schrump, D. S.; Butcher, D. O.; Raffeld, M.; Shoemaker, R. H. Gene expression profiling of alveolar soft-part sarcoma (ASPS). *BMC Cancer* **2009**, *9*, 22.

(5) Covell, D. G.; Wallqvist, A.; Kenney, S.; Vistica, D. T. Bioinformatic analysis of patient-derived ASPS gene expressions and ASPL-TFE3 fusion transcript levels identify potential therapeutic targets. *PLoS One* **2012**, *7* (11), e48023.

(6) Bisogno, G.; Rosolen, A.; Carli, M. Interferon alpha for alveolar soft part sarcoma. *Pediatr. Blood Cancer* **2005**, *44* (7), 687−688.

(7) Roozendaal, K. J.; de Valk, B.; ten Velden, J. J.; van der Woude, H. J.; Kroon, B. B. Alveolar soft-part sarcoma responding to interferon alpha-2b. *Br. J. Cancer* **2003**, *89* (2), 243−245.

(8) Kuriyama, K.; Todo, S.; Hibi, S.; Morimoto, A.; Imashuku, S. Alveolar soft part sarcoma with lung metastases. Response to interferon alpha-2a? *Med. Pediatr. Oncol.* **2001**, *37* (5), 482−483.

(9) Azizi, A. A.; Haberler, C.; Czech, T.; Gupper, A.; Prayer, D.; Breitschopf, H.; Acker, T.; Slavc, I. Vascular-endothelial-growth-factor (VEGF) expression and possible response to angiogenesis inhibitor bevacizumab in metastatic alveolar soft part sarcoma. *Lancet Oncol.* **2006**, *7* (6), 521−523.

(10) Mir, O.; Boudou-Rouquette, P.; Larousserie, F.; Blanchet, B.; Babinet, A.; Anract, P.; Goldwasser, F. Durable clinical activity of single-agent bevacizumab in a nonagenarian patient with metastatic alveolar soft part sarcoma. *Anticancer Drugs* **2012**, *23* (7), 745−748.

(11) Demetri, G. D.; van Oosterom, A. T.; Garrett, C. R.; Blackstein, M. E.; Shah, M. H.; Verweij, J.; McArthur, G.; Judson, I. R.; Heinrich, M. C.; Morgan, J. A.; Desai, J.; Fletcher, C. D.; George, S.; Bello, C. L.;

Huang, X.; Baum, C. M.; Casali, P. G. Efficacy and safety of sunitinib in patients with advanced gastrointestinal stromal tumour after failure of imatinib: a randomised controlled trial. *Lancet* **2006**, *368* (9544), 1329–1338.

(12) Stacchiotti, S.; Tamborini, E.; Marrari, A.; Brich, S.; Rota, S. A.; Orsenigo, M.; Crippa, F.; Morosi, C.; Gronchi, A.; Pierotti, M. A.; Casali, P. G.; Pilotti, S. Response to sunitinib malate in advanced alveolar soft part sarcoma. *Clin. Cancer Res.* **2009**, *15* (3), 1096–1104.

(13) Stacchiotti, S.; Negri, T.; Zaffaroni, N.; Palassini, E.; Morosi, C.; Brich, S.; Conca, E.; Bozzi, F.; Cassinelli, G.; Gronchi, A.; Casali, P. G.; Pilotti, S. Sunitinib in advanced alveolar soft part sarcoma: evidence of a direct antitumor effect. *Ann. Oncol.* **2011**, *22* (7), 1682–1690.

(14) Hanash, S. Progress in mining the human proteome for disease applications. *OMICS* **2011**, *15* (3), 133–139.

(15) Balgley, B. M.; Guo, T.; Zhao, K.; Fang, X.; Tavassoli, F. A.; Lee, C. S. Evaluation of archival time on shotgun proteomics of formalin-fixed and paraffin-embedded tissues. *J. Proteome Res.* **2009**, *8* (2), 917–925.

(16) von Lindern, M.; van Baal, S.; Wiegant, J.; Raap, A.; Hagemeijer, A.; Grosveld, G. Can, a putative oncogene associated with myeloid leukemogenesis, may be activated by fusion of its 3′ half to different genes: characterization of the set gene. *Mol. Cell. Biol.* **1992**, *12* (8), 3346–3355.

(17) Li, M.; Makkinje, A.; Damuni, Z. The myeloid leukemia-associated protein SET is a potent inhibitor of protein phosphatase 2A. *J. Biol. Chem.* **1996**, *271* (19), 11059–11062.

(18) Seshacharyulu, P.; Pandey, P.; Datta, K.; Batra, S. K. Phosphatase: PP2A structural importance, regulation and its aberrant expression in cancer. *Cancer Lett.* **2013**, *335* (1), 9–18.

(19) Kondo, T.; Hirohashi, S. Application of highly sensitive fluorescent dyes (CyDye DIGE Fluor saturation dyes) to laser microdissection and two-dimensional difference gel electrophoresis (2D-DIGE) for cancer proteomics. *Nat. Protoc.* **2006**, *1* (6), 2940–2956.

(20) Perrotti, D.; Neviani, P. Protein phosphatase 2A: a target for anticancer therapy. *Lancet Oncol.* **2013**, *14* (6), e229–e238.

(21) Perrotti, D.; Neviani, P. Protein phosphatase 2A (PP2A), a drugable tumor suppressor in Ph1(+) leukemias. *Cancer Metastasis Rev.* **2008**, *27* (2), 159–168.

(22) Yasui, H.; Hideshima, T.; Raje, N.; Roccaro, A. M.; Shiraishi, N.; Kumar, S.; Hamasaki, M.; Ishitsuka, K.; Tai, Y. T.; Podar, K.; Catley, L.; Mitsiades, C. S.; Richardson, P. G.; Albert, R.; Brinkmann, V.; Chauhan, D.; Anderson, K. C. FTY720 induces apoptosis in multiple myeloma cells and overcomes drug resistance. *Cancer Res.* **2005**, *65* (16), 7478–7484.

(23) Nagahara, Y.; Ikekita, M.; Shinomiya, T. T cell selective apoptosis by a novel immunosuppressant, FTY720, is closely regulated with Bcl-2. *Br. J. Pharmacol.* **2002**, *137* (7), 953–962.

(24) Matsumura, M.; Tsuchida, M.; Isoyama, N.; Takai, K.; Matsuyama, H. FTY720 mediates cytochrome c release from mitochondria during rat thymocyte apoptosis. *Transpl. Immunol.* **2010**, *23* (4), 174–179.

(25) Kayton, M. L.; Meyers, P.; Wexler, L. H.; Gerald, W. L.; LaQuaglia, M. P. Clinical presentation, treatment, and outcome of alveolar soft part sarcoma in children, adolescents, and young adults. *J. Pediatr. Surg.* **2006**, *41* (1), 187–193.

(26) *Soft Tissue Tumor Registry in Japan*, 2010.

(27) Kondo, T.; Hirohashi, S. Application of highly sensitive fluorescent dyes (CyDye DIGE Fluor saturation dyes) to laser microdissection and two-dimensional difference gel electrophoresis (2D-DIGE) for cancer proteomics. *Nat. Protoc.* **2007**, *1* (6), 2940–2956.

(28) Cervoni, N.; Detich, N.; Seo, S. B.; Chakravarti, D.; Szyf, M. The oncoprotein Set/TAF-1beta, an inhibitor of histone acetyltransferase, inhibits active demethylation of DNA, integrating DNA methylation and transcriptional silencing. *J. Biol. Chem.* **2002**, *277* (28), 25026–25031.

(29) Piazza, R.; Valletta, S.; Winkelmann, N.; Redaelli, S.; Spinelli, R.; Pirola, A.; Antolini, L.; Mologni, L.; Donadoni, C.; Papaemmanuil, E.; Schnittger, S.; Kim, D. W.; Boultwood, J.; Rossi, F.; Gaipa, G.; De Martini, G. P.; di Celle, P. F.; Jang, H. G.; Fantin, V.; Bignell, G. R.; Magistroni, V.; Haferlach, T.; Pogliani, E. M.; Campbell, P. J.; Chase, A. J.; Tapper, W. J.; Cross, N. C.; Gambacorti-Passerini, C. Recurrent SETBP1 mutations in atypical chronic myeloid leukemia. *Nat. Genet.* **2013**, *45* (1), 18–24.

(30) Ivaska, J.; Nissinen, L.; Immonen, N.; Eriksson, J. E.; Kahari, V. M.; Heino, J. Integrin alpha 2 beta 1 promotes activation of protein phosphatase 2A and dephosphorylation of Akt and glycogen synthase kinase 3 beta. *Mol. Cell. Biol.* **2002**, *22* (5), 1352–1359.

(31) Janssens, V.; Goris, J.; Van Hoof, C. PP2A: the expected tumor suppressor. *Curr. Opin. Genet. Dev.* **2005**, *15* (1), 34–41.

(32) Switzer, C. H.; Cheng, R. Y.; Vitek, T. M.; Christensen, D. J.; Wink, D. A.; Vitek, M. P. Targeting SET/I(2)PP2A oncoprotein functions as a multi-pathway strategy for cancer therapy. *Oncogene* **2011**, *30* (22), 2504–2513.

(33) Feschenko, M. S.; Stevenson, E.; Nairn, A. C.; Sweadner, K. J. A novel cAMP-stimulated pathway in protein phosphatase 2A activation. *J Pharmacol. Exp. Ther.* **2002**, *302* (1), 111–118.

(34) Neviani, P.; Santhanam, R.; Trotta, R.; Notari, M.; Blaser, B. W.; Liu, S.; Mao, H.; Chang, J. S.; Galietta, A.; Uttam, A.; Roy, D. C.; Valtieri, M.; Bruner-Klisovic, R.; Caligiuri, M. A.; Bloomfield, C. D.; Marcucci, G.; Perrotti, D. The tumor suppressor PP2A is functionally inactivated in blast crisis CML through the inhibitory activity of the BCR/ABL-regulated SET protein. *Cancer Cell* **2005**, *8* (5), 355–368.

(35) Matsuoka, Y.; Nagahara, Y.; Ikekita, M.; Shinomiya, T. A novel immunosuppressive agent FTY720 induced Akt dephosphorylation in leukemia cells. *Br. J. Pharmacol.* **2003**, *138* (7), 1303–1312.

(36) Perrotti, D.; Neviani, P. ReSETting PP2A tumour suppressor activity in blast crisis and imatinib-resistant chronic myelogenous leukaemia. *Br. J. Cancer* **2006**, *95* (7), 775–781.

(37) George, S.; Merriam, P.; Maki, R. G.; Van den Abbeele, A. D.; Yap, J. T.; Akhurst, T.; Harmon, D. C.; Bhuchar, G.; O'Mara, M. M.; D'Adamo, D. R.; Morgan, J.; Schwartz, G. K.; Wagner, A. J.; Butrynski, J. E.; Demetri, G. D.; Keohan, M. L. Multicenter phase II trial of sunitinib in the treatment of nongastrointestinal stromal tumor sarcomas. *J. Clin. Oncol* **2009**, *27* (19), 3154–3160.

dx.doi.org/10.1021/pr400929h | *J. Proteome Res.* XXXX, XXX, XXX–XXX

Proteomics & Bioinformatics

Mukaihara et al., J Proteomics Bioinform 2014, 7:6
http://dx.doi.org/10.4172/jpb.1000316

Research Article Open Access

Proteomic Profile of Epithelioid Sarcoma

Kenta Mukaihara[1,2], Daisuke Kubota[3], Akihiko Yoshida[4], Naofumi Asano[1], Yoshiyuki Suehara[2], Kazuo Kaneko[2], Akira Kawai[3] and Tadashi Kondo[1]*

[1]*Division of Pharmacoproteomics, National Cancer Center Research Institute, Tokyo, Japan*
[2]*Department of Orthopedic Surgery, Juntendo University School of Medicine, Tokyo, Japan*
[3]*Division of Musculoskeletal Oncology, National Cancer Center Hospital, Tokyo, Japan*
[4]*Pathology and Clinical Laboratory Division, National Cancer Center Hospital, Tokyo, Japan*

Abstract

Epithelioid sarcoma (ES) is a rare soft tissue sarcoma affecting young adults. It is a slow-growing tumor with a high rate of recurrence and metastasis to lymph nodes. Although deletion of the tumor suppressor gene, *SMARCB1/INI1*, has been identified in ES, the molecular background factors are largely unknown. To clarify the molecular aberrations contributing to the malignant features of ES, we investigated the proteins present in ES tumor tissues. Two-dimensional difference gel electrophoresis of homogenized tissue samples revealed 3363 protein spots, of which 91 showed differences in intensity between tumor and adjacent non-tumor tissues in eight ES cases. Using mass spectrometry, we characterized 69 unique proteins corresponding to these protein spots. We found that the complex histology of ES was obstacle for the investigation of molecular backgrounds of ES. For instance, although the higher expression of CAPZB in tumor tissues was confirmed by Western blotting, the immunohistochemistry did not determine the specific localize CAPZB in tumor cells. Our study demonstrated the possible utility of proteomic study, and at the same time the difficult aspect of proteomics using homogenized tissue samples.

Keywords: Epithelioid sarcoma; Proteomics; 2D-DIGE

Introduction

Epithelioid sarcoma (ES) is a soft tissue sarcoma affecting young adults [1]. ES is classified into two subtypes according the pathological observations: a classic form that often arises in the classic extremities as a slow-growing nodule [2], and a proximal form that tend to arise in deep areas of the pelvis, perineum, and genital tract [3]. Although the proximal form may have a more aggressive clinical course than the classic forms [4], the clinical courses are diverse, even for identical subtypes. Previous reports have focused on clinical and pathological prognostic factors associated with ES [3,5-7]. Recently, deletion of the *SMARCB1/INI1* tumor-suppressor gene (INI1) was reported in proximal-type ES [8], and loss of its expression was observed in approximately 90% of classic and proximal ES cases [9]. The tumorigenic properties of INI1 genetic inactivation have been reported [10], and loss of INI1 protein expression in ES has been shown to be due to epigenetic mechanisms of gene silencing by specific miRNAs [11]. As well as molecular studies of INI1, a large-scale immunohistochemical study has revealed that loss of INI1 expression had no prognostic impact on ES [4]. These reports suggest that there may be a molecular basis for differences in the clinical and pathological features of ES, and that further investigations to identify these aberrations might have clinical relevance.

To investigate the molecular basis of the malignant features of ES, previous studies have employed global molecular analysis. In a global gene expression study to identify the invasive potential of ES, Weber et al. carried out differential display RT-PCR with arbitrary primers using ES cell lines differing in their invasive potential, and found that expression of apoferritin light chain, GRU-1A, cytochrome *c* oxidase I, TI-227H, and ELISC-1 was associated with differences in invasiveness [12]. Using comparative genomic hybridization, Lushnikova et al. [13] examined DNA copy number changes in ES and reported recurrent gain at 11q13, and using immunohistochemistry confirmed overexpression of the cyclin D1 gene, located in 11q13. These studies suggested that a global molecular approach was effective, and that further investigations of a similar nature were warranted in ES. However, modern technology has not yet been applied for global molecular analysis of ES.

In the present study, to clarify the molecular background of ES, we adopted a proteomics approach using primary tumor tissues of ES. Proteomics can provide unique data that cannot be obtained using other global approaches. Using two-dimensional difference gel electrophoresis (2D-DIGE) and mass spectrometry [14], we identified proteins showing differential expression between tumor tissues and surrounding non-tumor tissues obtained from the ES patients.

Materials and Methods

Patients and tumor samples

This study included 8 patients with ES who were treated at the National Cancer Center Hospital between 1993 and 2013. Tumor and adjacent non-tumor tissues were obtained at the time of surgery, and stored in liquid nitrogen until use. Table 1 summarizes the patients' clinical and pathological information. This project was approved by the ethical review board of the National Cancer Center, and signed informed consent was obtained from all of the study patients.

Protein expression profiling

Proteins were extracted from frozen tissues as described previously [14]. In brief, tumor tissues were powdered with a Multi-beads shocker (Yasui Kikai, Osaka, Japan) in the presence of liquid nitrogen, and treated with urea lysis buffer (6 M urea, 2 M thiourea, 3% CHAPS, 1% Triton X-100). After centrifugation at 15,000 rpm for 30 min, the

***Corresponding author:** Tadashi Kondo, MD, PhD, Division of Pharmacoproteomics, National Cancer Center Research Institute, 5-1-1 Tsukiji, Chuo-ku, Tokyo 104-0045, Japan, Tel: +81-3-3542-2511; Fax: +81-3-3547-5298; E-mail: takondo@ncc.go.jp

Received May 20, 2014; **Accepted** June 19, 2014; **Published** June 24, 2014

Citation: Mukaihara K, Kubota D, Yoshida A, Asano N, Suehara Y, et al. (2014) Proteomic Profile of Epithelioid Sarcoma. J Proteomics Bioinform 7: 158-165. doi:10.4172/jpb.1000316

Case no.	Age	Gender	Location	Subtype	INI1 expression	Grade[a]	TNM stage [b]	Treatment	Local reccurence	Lymph node metastasis	Initial metastatic sites	Disease-free survival (months)	Overall survival (months)	Outcome
ES_1	29	F	Perineum	Classic	Negative	2	III	Curative surgery	Present	Absent	Lymph node	12	143	DOD
ES_2	52	M	Perineum	Proximal	Negative	2	IIA	Curative surgery	Present	Present	Lymph node	9	168	DOD
ES_3	36	M	Inguinal	Proximal	Negative	3	NA	Curative surgery	Present	Absent	Lung	25	113	DOD
ES_4	64	F	Back	Proximal	Positive	3	III	Curative surgery	Present	Absent	Lung	7	17	DOD
ES_5	32	M	Lower leg	Classic	Negative	3	III	Curative surgery	Absent	Absent	Lymph node	19	35	DOD
ES_6	48	F	Axilla	Proximal	Negative	3	IV	Palliative treatment	Present	NA	Lung	NA	4	DOD
ES_7	22	M	Foot	Classic	NA	2	IIA	Curative surgery	Absent	Absent	Bone	10	18	DOD
ES_8	41	M	Perineum	Classic	Negative	2	III	Curative surgery	Present	Present	Lymph node	10	19	DOD

NA: Data not available DOD: Dead of disease

[a]Modified FNCLCC (French Federation of Cancer Centers) system (Coindre et al. Cancer. 1986, 58: 306-309).

[b]Tumor-Nodes-Metastases Classification.

Table 1: Clinicopathologic features of ES samples.

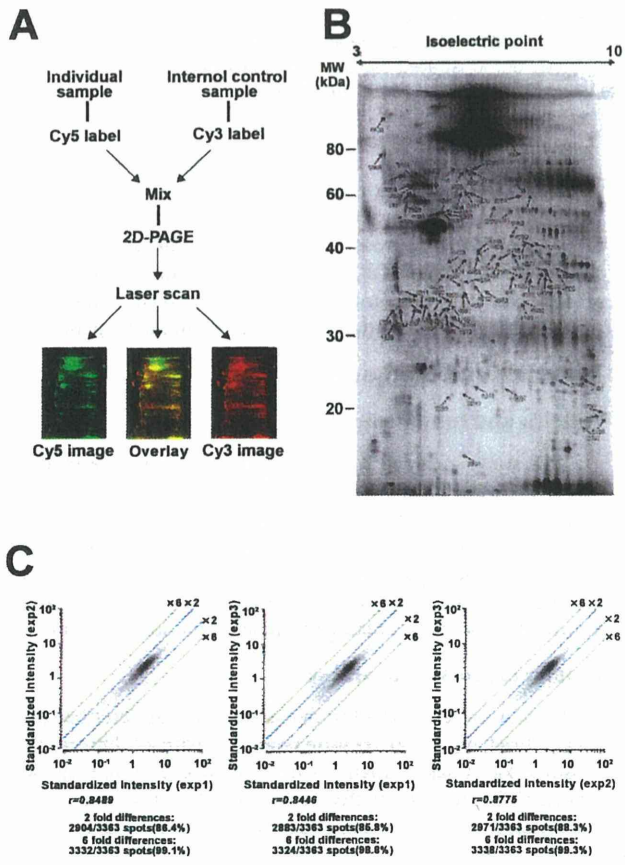

Figure 1: An overview of the experimental procedure for 2D-DIGE experiments with an internal control sample. A. The internal control and the individual sample are labeled with Cy3 and Cy5, respectively, mixed together, and separated by 2D-PAGE. After electrophoresis, the gel is laser-scanned, and the Cy3 and Cy5 images are obtained. The Cy5 image data are normalized with the Cy3 image data to compensate for any gel-to-gel variation. B. A typical gel image of the Cy3-labeled internal control sample. The spot numbers correspond to those in Figure 2 and Table 2. C. System reproducibility was evaluated by running the identical sample three times, and reproducibility was evaluated using a scattergram.

supernatant was recovered as the protein sample.

Protein expression profiling was performed by 2D-DIGE as described previously [14]. Figure 1A gives an overview of the 2D-DIGE protocol. In brief, the internal control sample was prepared by mixing together a small portion of the samples from all individuals. Five-microgram portions of the internal control sample and each individual sample were labeled with Cy3 and Cy5, respectively (CyDye DIGE Fluor saturation dye, GE Healthcare Biosciences, Uppsala, Sweden) [15,16]. The differently labeled protein samples were mixed, and then separated by two-dimensional gel electrophoresis. The first-dimension separation was achieved using Immobiline pH gradient DryStrip gels (24 cm long, pI range 3-10, GE Healthcare Biosciences) [17]. The second-dimension separation was achieved by SDS-PAGE using our original large-format electrophoresis apparatus (33-cm separation distance, Bio-craft, Tokyo, Japan) [14]. The gels were scanned using a laser scanner (Typhoon Trio, GE Healthcare Biosciences) at appropriate wavelengths for Cy3 and Cy5. For all protein spots, the Cy5 intensity was normalized against Cy3 intensity in the same gel using the ProgenesisSameSpots software package version 3 (Nonlinear Dynamics, Newcastle-upon-Tyne, UK), in order to compensate for gel-to-gel variations. All samples were examined in triplicate gels, and the mean normalized intensity value was used for comparative study.

Statistical analysis

Statistical comparisons were performed using the Expressionist software package (GeneData, Basel, Switzerland).

Protein identification by mass spectrometry

Mass spectrometric protein identification was performed as described previously [14]. In brief, 100 μg of the protein sample was labeled with Cy5, and separated by 2D-PAGE as described above. Protein spots were recovered from the gels using our original automated spot recovery device, and digested to tryptic peptides by in-gel digestion. The peptides were subjected to liquid chromatography coupled with nanoelectrospray tandem mass spectrometry (Finnigan LTQ Orbitrap mass spectrometer and LTQ linear ion trap mass spectrometer, Thermo Electron Co., San Jose, CA). The Mascot software package (version 2.2; Matrix Science, London, UK) and SWISS-PROT database (*Homo sapiens*, 471472 sequences in the Sprot-57.5.fasta file) were used for protein identification. Proteins with a Mascot score of 34 or more were considered to be positively identified.

Western blotting

Proteins were separated by SDS-PAGE and transferred to nitrocellulose membranes. Each membrane was incubated with mouse monoclonal antibody against CAPZB (1:500 dilution, Santa Cruz Biotechnology Inc, Santa Cruz, CA), and reacted with a horseradish

peroxidase-conjugated secondary antibody (1:1000 dilution, GE Healthcare Biosciences). The immunocomplex was detected using an enhanced chemiluminescence system (ECL Prime, GE Healthcare Biosciences), and the signal was monitored with a LAS-3000 laser scanner (FujiFilm, Tokyo, Japan). The membranes were then stained with 0.2% Ponceau S and 1% acetic acid (Sigma Aldrich, St. Louis, MO) [18,19], and the intensity of the protein bands was measured using the ImageQuant software package (GE Healthcare Biosciences). The intensity of individual protein bands was normalized against that of the entire lane.

Immunohistochemistry

Immunohistochemical examination was performed using formalin-fixed, paraffin-embedded tissues. In brief, paraffin sections of 4-μm thickness was cut from the representative block for each tumor and routinely deparaffinized. For INI1 staining, the sections were exposed to 3% hydrogen peroxide for 15 min to block endogenous peroxidase activity. The preparations were autoclaved in Targeted Retrieval Solution (Dako, Glostrup, Denmark) for antigen retrieval. The primary antibody used was INI1 (25/BAF47, 1:100; BD Biosciences, Franklin Lakes, NJ). The slides were incubated for 1 h at room temperature with the primary antibody and subsequently detected by the EnVision detection system with Linker (Dako). Diaminobenzidine was used as the chromogen, and hematoxylin as the counter stain. Complete loss of nuclear reactivity in the background of the non-neoplastic internal positive controls was regarded as deficient. For CAPZB staining, the slides were autoclaved in Tris-EDTA buffer (pH 9.0) at 121°C for 30 min and incubated with a commercial monoclonal antibody against CAPZB (1:500 dilution; Santa Cruz Biotechnology Inc.). Immunostaining was carried out by the streptavidin-biotin peroxidase method using a Strept ABC Complex/horseradish peroxidase kit (DAKO, Glostrup, Denmark).

Results and Discussion

In order to develop clinical applications that can improve the outcome of patients with ES, it has been necessary to clarify the molecular basis of ES malignancy. The recent advent of global protein expression technologies has enabled comprehensive analysis of molecular aberrations in tumor cells, and a tremendous amount of data that may lead to clinical applications has been generated. However, the proteomic approaches have not been applied to ES, probably because of its relative rarity and the fact that clinical materials for basic research are in short supply.

In this study, we conducted a proteomic comparison between tumor and non-tumor tissues in ES. This is the first report of a proteomics approach to ES. Identification of proteins showing unique expression in tumor tissues is the first step toward clarifying the molecular basis of tumor biology. The differences between tumor and non-tumor tissues may include alterations that have occurred during carcinogenesis, or during cancer progression, and reflect the various features of malignancy including invasion, metastasis and resistance to therapy. Such a simple comparison of tumor tissues with normal ones may not in itself yield significant results, because the surrounding non-tumor tissues are not normal counterparts of tumor tissues in ES. However, investigation of the proteins identified may further our understanding of the molecular backgrounds of ES.

Here we employed 2D-DIGE to investigate the proteomic background of ES. 2D-DIGE is an advanced version of 2D-PAGE, which has been widely used to examine protein expression profiles since 1975. Although 2D-PAGE has been used for protein research for an exceptionally long period, it has a number of inherent drawbacks, one of which is gel-to-gel variations. We attempted to resolve this issue using a common internal control sample in 2D-DIGE (Figure 1A), and thus successfully compensated for any gel-to-gel variations (Figure 1C). Generally, the separation performance of gel-based proteomics parallels the separation distance achieved by electrophoresis. For longer separation distance, we developed our original large-format electrophoresis apparatus, and we successfully observed 3363 protein spots using it (Figure 1B). In 2D-DIGE, proteins are detected by laser scanning of the gels sandwiched between low-fluorescence glass plates. Therefore, a gel as large as the laser scanning area can be used without any risk of breaking the fragile polyacrylamide gel. The higher separation performance may also contribute to the high reproducibility of protein expression profiling (Figure 1C). When we ran an identical sample three times independently, the intensity of at least 85.8% of 3363 protein spots observed was scattered within a difference of two-fold, and showed a relative correlation of at least 0.84. As the intensity of at least 98.8% of the 3363 protein spots was scattered within a six-fold difference range, we further examined spots that showed more than a six-fold difference in intensity between tumor and non-tumor tissues. The intensities of all 3363 protein spots are summarized in Supplementary Table 1.

We identified 91 protein spots whose intensity differed significantly ($p<0.01$, >6-fold ratio of means) between tumor and non-tumor tissues. These 91 spots are localized on the 2D image shown in Figure 1B. The normalized and averaged intensity of the 91 spots is shown in the form of a heat map in Figure 2, which was created using the data in Supplementary Table 1. Mass spectrometric protein identification revealed that the 91 protein spots corresponded to 69 distinct gene products (Figure 2 and Table 2). Generally, gene products are modified after transcription and translation, and single genes can generate multiple protein forms. Thus, the molecular events that had given rise to the multiple protein forms of these 69 genes, and how they differed between tumor and non-tumor tissues, were clearly of interest. Supplementary Table 2 summarizes the supporting data used for identification of these proteins. Generally, proteome data are biased by proteomics technologies, and we observe what we can observe in given technical conditions. As only proteins with differential expression were subjected to mass spectrometric protein identification, we cannot evaluate the limitation of 2D-DIGE. However, 2D-DIGE in this study clearly has limitation. For example, only the proteins with pI ranging between 4 and 7 were included in this study, and the proteins with pI higher than 7 were not considered. Moreover, the proteins with low expression level such as transcription factors may not be included either. Indeed, we didn't identify the products of SMARCB1/INI1, whose unique expression was reported in ES. Generally, proteomics modalities also have their own technical limitations, and there is no almighty proteomics modality. Therefore, the combined use of multiple proteomics modalities is required for comprehensive protein expression study. We demonstrated the presence of proteins with differential expression between tumor and non-tumor tissues using 2D-DIGE, and we hope that our proteomic study facilitates further investigation of ES at the protein level.

Among them, we examined the differential expression of CAPZB [20], which was up-regulated in ES tumor tissues (Figure 2 and Table 2). CAPZB is a member of the F-actin capping protein family, which bind the barbed ends of actin and regulate cell morphology and cytoskeletal organization [21]. Although CAPZB has been reported in human salivary gland cancer [22], its roles in other types of cancer have not